Jour. Fac. Sci., Hokkaido Univ., Ser. VII (Geophysics), Vol. 9, No. 4, 415-427, 1994.

Spectral Shape of Acceleration at High Frequencies: Attenuation and Site Effect

Abbas Mahdavian and Tsutomu Sasatani

Department of Geophysics, Faculty of Science, Hokkaido University, Sapporo 060, Japan

(Received November 30, 1993)

Abstract

We study the spectral shape of acceleration for strong motion seismograms at the rock and sedimentary sites from earthquakes occurring along the Pacific coast of Hokkaido. At high frequencies, the acceleration spectrum decays exponentially at both sites and the decay parameter, κ, is obtained. On the average, κ values at the rock site are smaller than those at the sedimentary site. κ values show a slight increase with hypocentral distance. Under the assumption of the omega-squared source model, we interpret these results based on a two zone attenuation model: near surface (site effect) and regional attenuation.

1. Introduction

The shape and amplitude of the Fourier amplitude spectrum of strong ground acceleration contains fundamental information about physical processes at the earthquake source and wave propagation in the crust of the earth. According to the idealization of the omega-squared source model (e.g., Aki, 1967), S-wave acceleration spectra should be flat at frequencies greater than f_0, the corner frequency. Observationally, however, this is rarely the case. Hanks (1982) suggests that, in general, the acceleration spectrum is flat above the corner frequency to a second corner frequency (f_{max}) above which the spectrum decays abruptly. He considers that f_{max} is controlled by local site conditions, but Papageorgiou and Aki (1983) suggest that f_{max} is controlled by source properties. On the other hand, Anderson and Hough (1984) have proposed a different model of the S-wave acceleration spectra; the spectra at high frequencies ($f > f_0$) fall off exponentially. They suggest that the exponential decay is related to attenuation within the earth.

In this paper, we study the spectral shape of acceleration at high frequencies

for earthquakes occurring along the Pacific coast of Hokkaido. Through an examination of the observed spectral shape, we have come to the conclusion that the Anderson and Hough's parametric shape is preferable. Then we obtain the spectral decay parameters and explain them with attenuation model in the crust and upper mantle.

2. Data

We analyzed strong motion seismograms observed at MYR (Moyori) and OBI (Obihiro); MYR is located on the rock site at the edge of the Tokachi plain, and OBI, on the sedimentary site at the central part of the Tokachi plain (Sasatani et al., 1990; Fig. 1a). These seismograms were obtained by the wide frequency band instruments, a velocity type strong motion seismometer with a flat response from 0.002 to 20 Hz (Muramatu, 1977; Fig. 1b). The signals were digitized by a sampling frequency of 50 Hz and with a dynamic range of 16 bit. A corner frequency of anti-alias filter is set at 20Hz. The wide frequency band instrument is necessary to obtain reliable spectra.

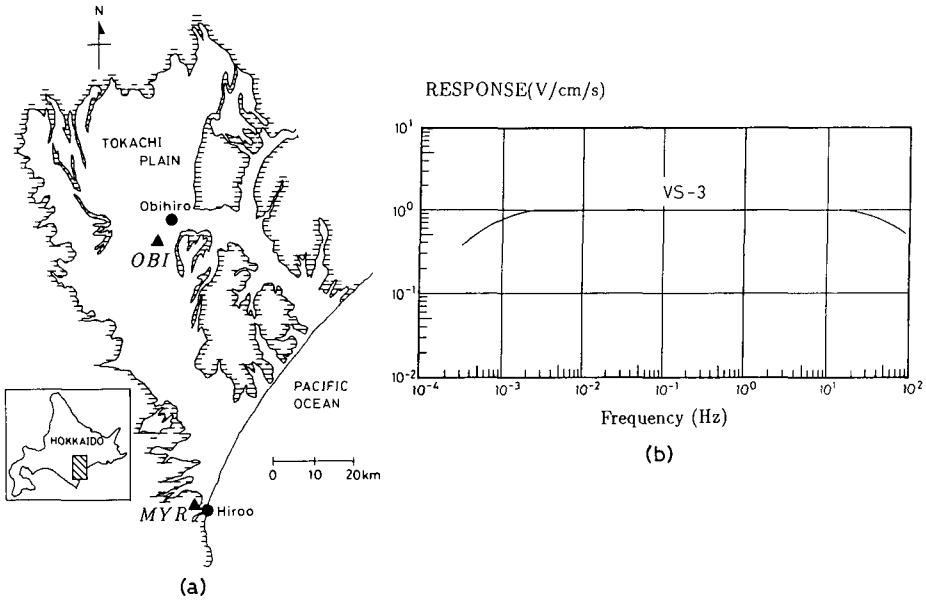

Fig. 1. (a) Simplified geological map of the Tokachi plain (after Geological Survey of Hokkaido, 1980). This plain is covered mainly by Terrace deposits. MYR and OBI stations are also shown. (b) Frequency characteristics of the velocity-type strong motion seismometer (Muramatu, 1977).

We studied S-wave spectra for horizontal components from about 30 earthquakes occurring along the Pacific coast of Hokkaido and having magnitudes of 4 to 6.4. Figure 2a shows epicentral distribution of analyzed earthquakes. The earthquake information is given in Tables 1 and 2. These have depths from 60 to 80 km as shown in Fig. 2b.

3. S-wave spectra of acceleration

The acceleration seismograms were obtained by differentiating velocity seismograms in the frequency domain using the Fourier transform. We selected the S-wave portion which has a significant duration in the acceleration seismograms, by using the Husid plot method (Dobry et al., 1978). Sample data were windowed by 10 percent cosine tapering at both ends, and S-wave Fourier spectra of acceleration were computed for horizontal components. The S-wave portion may be contaminated by P coda. Then, we first compared the spectra of P coda and S-waves to check a signal-to-noise (P coda) ratio. In this analysis, we used seismograms with a high signal-to-noise ratio.

Now we examine the shape of the Fourier spectrum of S-wave acceleration based on Fig. 3. By the shape of a spectrum we refer to a smooth trend through the spectrum: the fine structure which is superimposed on this trend is not

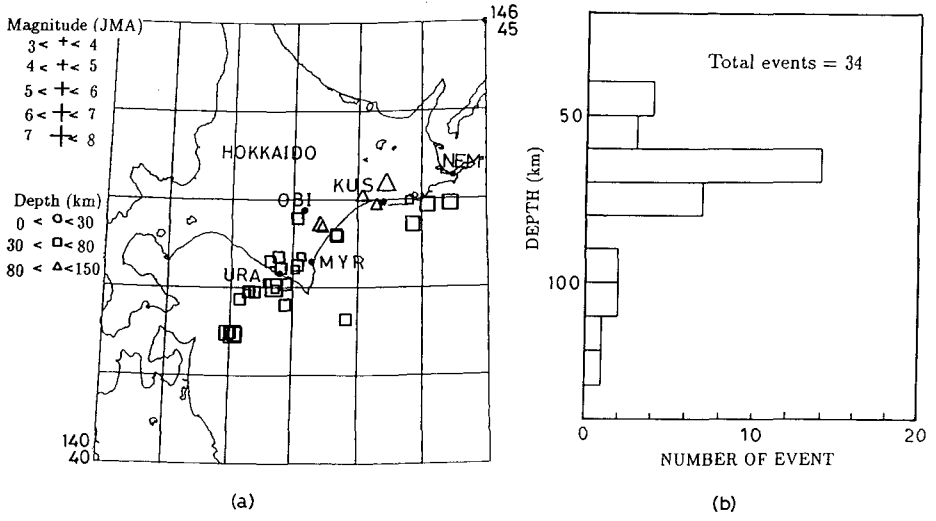

Fig. 2. (a) Epicentral distribution of earthquakes analyzed in this study. (b) Depth distribution of analyzed earthquakes.

meant to be included. At low frequencies the spectrum increases with frequencies ($\sim f^2$); this trend fits the omega-squared model. The spectrum is not flat at high frequencies, but it decreases with frequencies. This trend differs from the omega-squared model as mentioned in Introduction. There is no apparent slope break at frequencies higher than about 2 Hz. We need not pick out the f_{max} above which the spectrum decays abruptly (Hanks, 1982): the

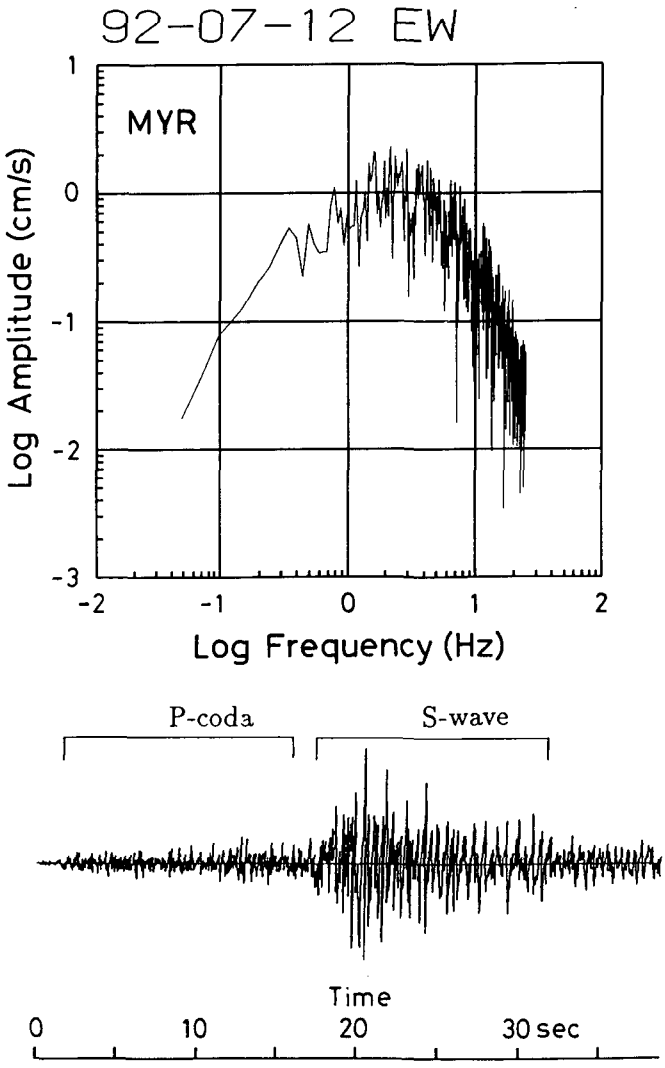

Fig. 3. S-wave spectrum of acceleration for the July 12, 1992 earthquake (M6.3).

spectral decay is rather smooth as proposed by Anderson and Hough (1984).

Figure 4 shows several S-wave spectra which have the same trend as mentioned above. Then we have come to the conclusion that Anderson and Hough's parameterization is a reasonable one.

4. High frequency decay parameter, κ

Anderson and Hough (1984) hypothesized the acceleration spectrum $A(f)$ at high frequencies as

$$A(f)=A_0 \exp(-\pi\kappa f) \quad \text{for } f>f* \tag{1}$$

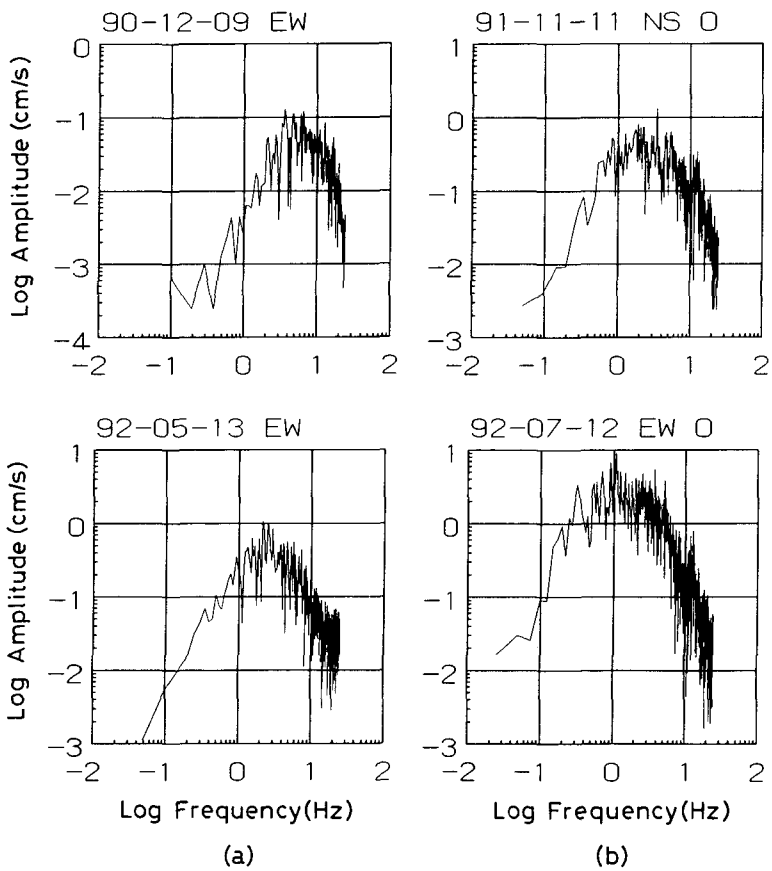

Fig. 4. An example of S-wave spectra. (a) MYR and (b) OBI.

where A_0 depends on source properties, epicentral distance, and perhaps other factors ; $f*$ is chosen as the point where decay begins, usually from 1 to several Hz ; and κ is used to parameterize the decay in the high frequency band. This formula shows the linear decay on log-linear plot of the spectrum as shown in Fig. 5. The spectrum was fitted to a straight line using a least-squares approach over the chosen frequency band and κ was estimated from the slope. We did not compute error bars for κ value because the variance of the regression is highly dependent on the fine structure superimposed on the overall trend of the spectrum.

The initial effort was focused on choosing the frequency band in which the spectrum shows the evident linear decay on log-linear plot. The upper limit was set at the frequency where the signal reached the noise level. The choice of the lower limit, $f*$, requires greater caution : sometimes $f*$ is not so clear. We can see how different values of $f*$ produce the χ value fluctuation (about 30 percent) in Fig. 6.

Figure 7 shows an example of the S-wave spectra which fit well the linear decay on log-linear plot. κ values obtained are summarized in Tables 1 and 2 for MYR and OBI. On the average, κ values for MYR are smaller than those for OBI : the average values are 0.045 ± 0.0136 for MYR and 0.0605 ± 0.0176 for OBI.

We examine the κ value dependence on focal depth, azimuth or source location, magnitude and distance. Figure 8 shows κ values versus focal depth,

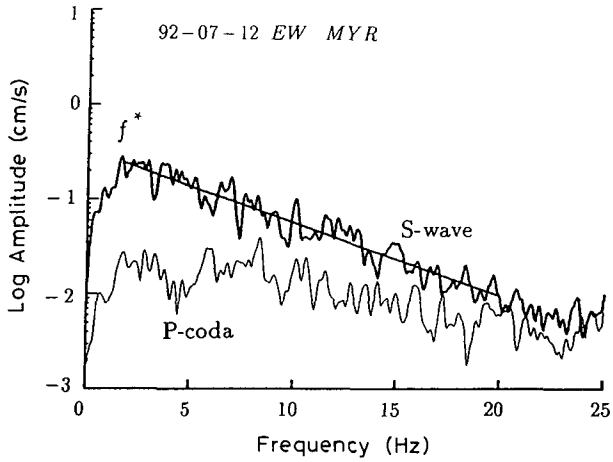

Fig. 5. S-wave spectrum of acceleration on log-linear plot for the July 12, 1992 earthquake (M6.3). At high frequencies, the S-wave spectrum decays linearly as shown by a straight line. $f*$ is the lower limit of the frequency band in which the spectrum shows the evident linear decay. Also shown is P-coda spectrum.

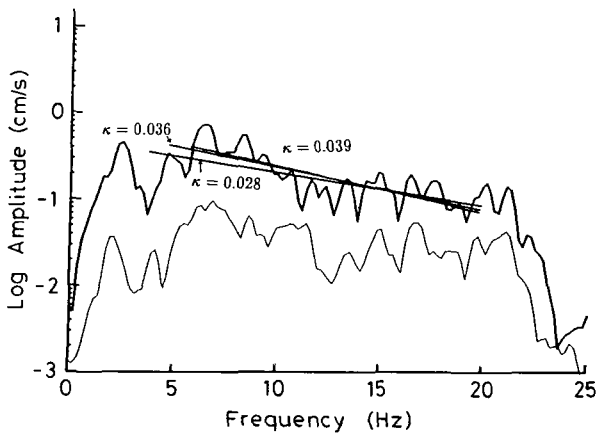

Fig. 6. Fluctuation of κ estimation for different lower limits ($f*$).

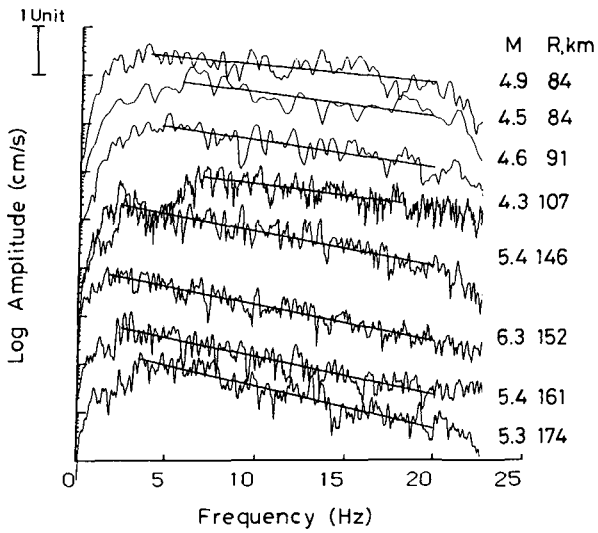

Fig. 7. An example of S-wave spectra of acceleration on log-linear scale. Superimposed on each spectrum is a linear least-squares fit over the frequency band up to 20Hz. Earthquake size (M) and hypocentral distance (R) are indicated on right of each spectrum.

azimuth and magnitude for MYR and OBI. Fluctuations in these figures appear to be randomly distributed, indicating no evident dependence of κ values on focal depth, azimuth and magnitude.

Figure 9 shows κ values as a function of hypocentral distance for MYR and OBI. We can say that κ values slightly increase with hypocentral distances.

Table 1. Spectral decay parameters (κ) for accelerograms recorded at MYR. The table also shows the date, focal depth (H), magnitude (M in JMA scale), hypocentral distance (R), and station-to-epicenter azimuth ($Az.$ in degree) of analyzed earthquakes.

No.	Date	H(km)	M	R(km)	$Az.$	κ(EW)	κ(NS)
1	90 DEC. 9	117.0	4.3	157.6	36.8	0.036	0.021
2	90 DEC. 10	44.0	5.1	196.4	66.8	0.051	0.052
3	90 DEC. 25	68.0	4.9	107.9	243.3	0.066	0.055
4	90 DEC. 28	64.0	4.9	152.6	229.9	0.061	0.052
5	91 FEB. 26	96.0	4.3	107.0	16.3	0.044	0.035
6	91 APR. 24	52.0	5.4	146.0	69.3	0.054	0.045
7	91 JUN. 13	123.0	6.0	132.8	12.1	0.027	0.022
8	91 JUN. 17	69.0	3.8	94.1	245.4	0.036	0.035
9	91 JUN. 20	61.0	4.1	88.5	211.6	0.046	0.042
10	91 JUN. 23	67.0	4.8	124.7	243.6	0.061	0.061
11	91 JUN. 27	73.0	4.6	115.8	245.3	0.080	0.050
12	91 SEP. 27	70.0	4.5	83.7	44.9	0.039	0.039
13	91 OCT. 18	56.0	5.3	173.8	63.7	0.064	0.053
14	91 OCT. 18	67.0	4.0	114.8	245.0	0.055	0.043
15	91 OCT. 25	104.0	6.1	172.5	42.4	0.046	0.045
16	91 OCT. 28	65.0	4.2	86.8	341.7	0.049	0.030
17	91 NOV. 2	62.0	4.0	158.3	57.6	0.048	0.037
18	91 NOV. 8	73.0	4.6	90.7	271.2	0.043	0.034
19	91 NOV. 27	67.0	6.4	88.8	236.4	0.047	0.047
20	91 DEC. 3	56.0	3.7	80.8	233.7	0.053	0.041
21	91 DEC. 18	65.0	4.0	69.1	244.1	0.031	0.011
22	92 JAN. 12	44.0	4.0	46.2	297.0	0.050	0.014
23	92 JAN. 13	41.0	4.7	59.4	228.2	0.041	0.053
24	92 JAN. 17	75.0	5.4	161.2	231.4	0.060	0.061
25	92 JAN. 23	80.0	4.2	91.0	278.7	0.030	0.029
26	92 JAN. 26	49.0	4.2	98.4	149.0	0.042	0.040
27	92 FEB. 14	77.0	4.2	87.2	258.4	0.049	0.047
28	92 MAR. 2	71.0	4.8	112.6	243.7	0.071	0.042
29	92 APR. 7	72.0	4.9	84.0	46.3	0.030	0.033
30	92 APR. 20	62.0	5.0	63.8	256.4	0.047	0.024
31	92 JUL. 12	65.0	6.3	152.1	228.6	0.057	0.053
32	92 JUL. 13	71.0	5.3	153.0	227.6	0.067	0.065

Average value = 0.045 ± 0.0136

Table 2. Spectral decay parameters (κ) for accelerograms recorded at OBI. The table also shows the date, focal depth (H), magnitude (M in JMA scale), hypocentral distance (R), and station-to-epicenter azimuth ($Az.$ in degree) of analyzed earthquakes.

No.	Date	H(km)	M	R(km)	$Az.$	κ(EW)	κ(NS)
1	91 APR. 24	52.0	5.4	147.4	96.9	0.068	0.067
2	91 JUN. 13	123.0	6.0	125.6	128.7	0.056	0.045
3	91 JUN. 23	67.0	4.8	155.5	217.1	0.070	0.076
4	91 AUG. 16	69.0	4.8	100.4	191.3	0.052	0.052
5	91 SEP. 2	65.0	5.0	92.7	182.9	0.056	0.053
6	91 SEP. 27	70.0	4.5	87.7	127.9	0.039	0.047
7	91 OCT. 25	104.0	6.1	150.3	70.2	0.060	0.076
8	91 OCT. 28	65.0	4.2	66.4	219.8	0.045	0.045
9	91 NOV. 11	63.0	4.8	141.2	217.2	0.038	0.042
10	91 NOV. 27	67.0	6.4	124.5	201.9	0.100	0.100
11	92 JAN. 13	41.0	4.7	104.7	193.5	0.043	0.049
12	92 JAN. 17	75.0	5.4	199.5	213.5	0.067	0.068
13	92 MAR. 2	71.0	4.8	144.0	215.6	0.051	0.051
14	92 APR. 7	72.0	4.9	91.4	127.2	0.070	0.096
15	92 APR. 20	62.0	5.0	97.1	187.2	0.049	0.043
16	92 JUL. 12	65.0	6.3	193.3	210.9	0.079	0.083

Average value $=0.0605\pm0.0176$

We have no reasonable basis to describe the distance dependence of κ values. Thus we tentatively assumed a simple linear dependence of κ on distances (Anderson and Hough, 1984) and obtained as

$$\kappa(R)=0.029+0.00014R \quad \text{for MYR} \tag{2}$$

$$\kappa(R)=0.037+0.00019R \quad \text{for OBI} \tag{3}$$

where R is the hypocentral distance in km.

5. Discussion and conclusions

We found that at high frequencies the Fourier acceleration spectra of S-waves decay exponentially for earthquakes occurring along the Pacific coast of Hokkaido. The decay parameters, κ values, show a slight increase with hypocentral distances. The same results have been obtained in El-Centro and San Fernando of California (Anderson and Hough, 1984), near Anza of California (Hough et al., 1988), and Guerrero subduction zone of Mexico (Humphrey and Anderson, 1992). However, the distance dependence varies from region to

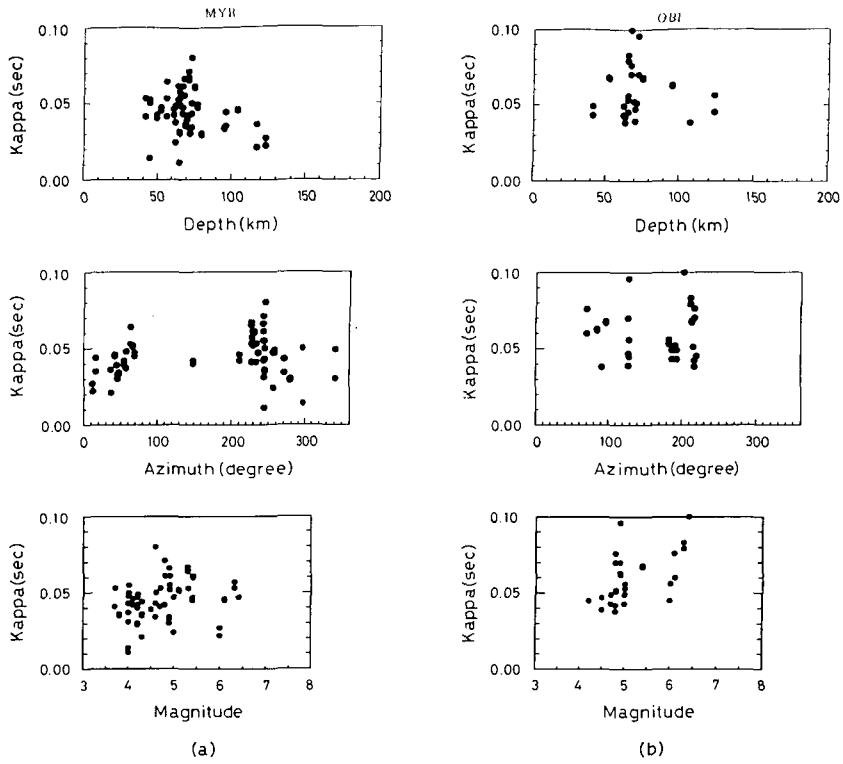

Fig. 8. κ values versus focal depth, azimuth and magnitude. (a) MYR and (b) OBI.

region. On the other hand, Rovelli et al. (1988) have found no clear distance dependence of κ values in Italy. These studies indicate a regional variation of distance dependence of κ values and make a simple interpretation of κ values rather difficult.

We interpret the linear dependence of κ values on hypocentral distances, following Anderson and Hough (1984) and Hough et al. (1988). A two zone model for crust-upper mantle structure is assumed: the upper surface zone with a thickness of H km and a quality factor of $Q_{(1)}$ and the lower zone with a quality factor of $Q_{(2)}$ where the lateral propagation (distance of R km) mostly takes place. For this model we may write:

$$\kappa \sim \frac{H}{Q_{(1)} V_{s1}} + \frac{R}{Q_{(2)} V_{s2}} \tag{4}$$

where V_{s1} and V_{s2} are S-wave velocities in the upper and lower zones.

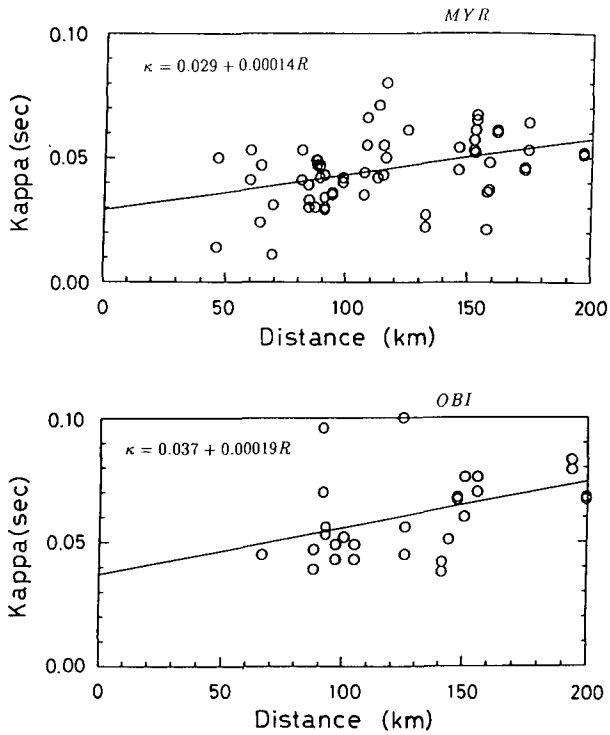

Fig. 9. κ values as a function of hypocentral distance. Upper: MYR and lower: OBI. A thick line in each figure shows the least-squares fit of data set.

Comparing this with formulae (2) and (3), we may interpret that $\kappa(0)$ in (2) and (3) represents a site effect due to attenuation in the sedimentary and weathered layers.

From (2) and (3), $\kappa(0)$ for MYR located on the rock site is smaller than $\kappa(0)$ for OBI located on the sedimentary site. Thus a difference of $\kappa(0)$ for MYR and OBI may represent attenuation in the sedimentary layer in the Tokachi plain. If we assume $V_{s1} \sim 0.8$ km/sec and $H = 0.6$ km based on Matsushima and Okada's study (1990), the difference of $\kappa(0)$ for MYR and OBI gives Q value of about 90 for the sedimentary layer. Since we have no data for hypocentral distances less than 40 km as shown in Fig. 9, $\kappa(0)$ estimation may be not so accurate. If we use a difference of the average values for MYR and OBI (Tables 1 and 2) instead of the $\kappa(0)$ difference, we obtain Q value of about 50 for the sedimentary layer. These values are fairly large compared with Q value for the upper sedimentary layer in the Los Angeles basin (e.g., Hauksson et al.,

1987), but approximately the same as an average Q value (about 70) in the sedimentary layer in the Kanto plain (Kinoshita, 1992).

The slope, dx/dR in (2) and (3), is a regional effect which describes whole path attenuation during lateral propagation. Assuming $V_{s2}=4.5$ km/sec, we obtain $Q_{(2)}$ of about 1400 from the average value of dx/dR ($=0.000165$ sec/km). This value is somewhat larger than Q values for the crust-upper mantle beneath the Pacific coast in the Tohoku region (Umino and Hasegawa, 1984).

In above interpretation, we assume frequency independent Q in the crust and upper mantle. However, Mahdavian and Sasatani (1992) obtained the frequency dependent Q around Hokkaido. One plausible explanation would be to appeal to models in which total Q_t is separated into two components as

$$\frac{1}{Q_t}=\frac{1}{Q_i}+\frac{1}{Q_d}$$

where Q_i is a frequency-independent component and Q_d, a frequency-dependent component. In this model, if Q_d is proportional to f, attenuation does not affect the spectral decay parameter $\varkappa$ (Fig. 13 in Anderson and Hough, 1984).

We have no information about the underground structure at MYR. We assume that MYR is located on the rock site, but the $\varkappa(0)$ or the average value of $\varkappa$ values is not so small compared with that for OBI on the sedimentary site. This means that even on the rock site, near surface attenuation effect exists (e.g., Cranswick et al., 1985).

A simple interpretation of the $\varkappa$ value dependence on distances and the Q values obtained above are merely tentative. It may be reasonable to conclude that the $\varkappa$ effect represents the high frequency decay of S-wave acceleration spectrum, including the total effects of near surface and regional attenuation.

Acknowledgments

The maintenance of strong motion observation at MYR and OBI have been carried out by us and Dr. Mitsuko Furumura of our laboratory and Professor Toshiro Koyanagi of Obihiro University of Agriculture and Veterinary Medicine. This work could not have been performed without the kind help of them.

References

Aki, K., 1967. Scaling law of seismic spectrum. J. Geophys. Res., **72**, 1217-1231.

Anderson, J.G. and S. Hough, 1984. A model for the shape of the Fourier amplitude spectrum of acceleration at high frequencies. Bull. Seism. Soc. Am., **74**, 1969-1994.

Cranswick, E., R. Wetmiller and J. Boatwright, 1985. High-frequency observations and source parameters of micro-earthquakes recorded at hard-rock sites. Bull. Seism. Soc. Am., **75**, 1535-1567.

Dobry, R., M. Idriss and E. Ng, 1978. Duration characteristics of horizontal components of strong-motion earthquake records. Bull. Seism. Soc. Am., **68**, 1487-1520.

Geological Survey of Hokkaido, 1980. Geological map (1 : 600000).

Hanks, T.C., 1982. f_{max}. Bull. Seism. Soc. Am., **72**, 1867-1879.

Hauksson, E., T. Teng and T.L. Henyey, 1987. Results from a deep seismometer array : site response, low Q values, and f_{max}. Bull. Seism. Soc. Am., **77**, 1883-1904.

Hough, S.E., J.G. Anderson, J. Brune, F. Vernon, III, J. Berger, J. Fletcher, L. Haar, T. Hanks and L. Baker, 1988. Attenuation near Anza, California. Bull. Seism. Soc. Am., **78**, 672-691.

Humphrey, J.R. and J.G. Anderson, 1992. Shear-wave attenuation and site response in Guerrero, Mexico. Bull. Seism. Soc. Am., **82**, 1622-1645.

Kinoshita, S., 1992. Frequency dependent attenuation of shear waves in a sedimentary layers-basement system in the Kanto area, Japan. Proc. Int. Symposium on Earthquake Disaster Prevention, CENAPRED, Mexico, Vol. **1**, 212-226.

Mahdavian, A. and T. Sasatani, 1992. Strong ground motion from the Urakawa earthquake of Jan. 25, 1989. J. Fac. Sci. Hokkaido Univ., Ser. VII (Geophys.), **9**, 253-267.

Matsushima, T. and H. Okada, 1990. Determination of deep geological structures under urban areas using long-period microtremors. Butsuri-Tansa, **43**, 21-33.

Muramatu, I., 1977. A velocity type strong motion seismograph with wide frequency range. Zisin, **30**, 317-338 (in Japanese).

Papageogiou, A.S. and K. Aki, 1983. A specific barrier model for the quantitative description of inhomogeneous faulting and the prediction of strong ground motion, Part II. Application of the model. Bull. Seism. Soc. Am., **73**, 953-978.

Rovelli, A., O. Bonamassa, M. Cocco, M.D. Bona and S. Mazza, 1988. Scaling laws and spectral parameters of the ground motion in active extensional areas in Italy. Bull. Seism. Soc. Am., **78**, 530-560.

Sasatani, T., T. Matsushima and T. Koyanagi, 1990. Observation of strong ground motion in and around the Tokachi plain. Geophys. Bull. Hokkaido Univ., **54**, 15-22 (in Japanese).

Umino, N. and A. Hasegawa, 1984. Three-dimensional Qs structure in the northeastern Japan arc. Zisin, **37**, 217-228 (in Japanese).